

Advances and prospects in nitrides based light-emitting-diodes*

Li Jinmin(李晋闽)^{1, 2, 3, †}, Liu Zhe(刘喆)^{1, 2, 3}, Liu Zhiqiang(刘志强)^{1, 2, 3},
 Yan Jianchang(闫建昌)^{1, 2, 3}, Wei Tongbo(魏同波)^{1, 2, 3}, Yi Xiaoyan(伊晓燕)^{1, 2, 3},
 and Wang Junxi(王军喜)^{1, 2, 3}

¹Research and Development Center for Solid State Lighting, Institute of Semiconductors, Chinese Academy of Sciences, Beijing 100083, China

²State Key Laboratory of Solid State Lighting, Beijing 100083, China

³Beijing Engineering Research Center for the 3rd Generation Semiconductor Materials and Application, Beijing 100083, China

Abstract: Due to their low power consumption, long lifetime and high efficiency, nitrides based white light-emitting-diodes (LEDs) have long been considered to be a promising technology for next generation illumination. In this work, we provide a brief review of the development of GaN based LEDs. Some pioneering and significant experiment results of our group and the overview of the recent progress in this field are presented. We hope it can provide some meaningful information for the development of high efficiency GaN based LEDs and solid-state-lighting.

Key words: nitrides; light-emitting-diodes; MOCVD; multiple-quantum-well; p-doping

DOI: 10.1088/1674-4926/37/6/061001

PACS: 42.55.Px

1. Introduction

Compared with traditional incandescent and fluorescent lamps, nitrides based white light-emitting-diodes (LEDs) are considered to be a promising technology for next generation illumination due to their low power consumption, long lifetime and high efficiency.

The emitting of blue light proved to be a difficult task, which took three more decades to achieve. The efforts on this topic could be tracked back to the 1950s^[1]. At the end of the 1950s, the possibility of a new lighting technology using GaN was considered by Philips Research Laboratories. The photoluminescence of GaN power was obtained by Grimmeiss and Koelmans. The first single-crystal film of GaN was prepared by Maruska and Tietjen using the HVPE technique in 1969. In the 1970s, new crystal growth techniques, MBE (molecular beam epitaxy) and MOVPE (metal organic vapor phase epitaxy) were developed. Since then, several technical breakthroughs enabled single-phase growth of wurtzite GaN and In-GaN. A major problem for manufacturing p-n junctions was the difficulty to p-dope GaN. At the end of the 1980s, Amano, Akasaki and co-workers made an important conductivity control of p-type GaN by low energy electron irradiation. Later, Nakamura demonstrated that a simple thermal treatment (annealing) leads to efficient activation of Mg acceptors. It was an important breakthrough and opened the way to p-n junctions in GaN. Another crucial step in developing efficient blue LEDs was the growth of alloys (AlGaN, InGaN), which are necessary to produce hetero junctions. Such hetero junctions were realized in the early 1990s by Akasaki's and Nakamura's research groups. In 1994, Nakamura and co-workers achieved a quantum efficiency of 2.7% using a double hetero junction InGaN/AlGaN. With these important first steps, the path was

cleared towards the development of efficient blue LEDs and their application was open^[2]. Today's efficient LEDs are the result of a long series of breakthroughs in basic materials physics and crystal growth, in device physics with advanced hetero structure design, and in optical physics for the optimization of the light out-coupling. The historical development of blue, green, red and "white" LEDs is summarized in the picture below.

Over the last several decades, a long series of breakthroughs in basic materials physics, crystal growth, hetero structure design, device physics has been achieved to optimize the efficiency of GaN-based LEDs. As a result, the efficiency of GaN based LEDs improved dramatically (as shown in Figure 1)^[3]. Today, GaN-based LEDs provide the dominant technology for general lighting and back-illuminated liquid crystal displays, and their application will continue to expand to many novel fields. In this work, some pioneering and significant experiment results of our group and the overview of the recent progress in GaN based LEDs are presented. We hope it can provide some meaningful information for the development of high efficiency GaN based LEDs.

2. Advances in GaN based LEDs

2.1. High Al composition AlGaN layers on nano-patterned sapphire substrate and efficient DUV-LEDs^[4]

AlGaN based ultraviolet (UV) LEDs promise to provide a good solution for SLL of high color rendering. It is also hoped that efficient deep UV LEDs would provide more energy efficient compact solutions compared with the present fragile and hazardous mercury vapor lamps. Proposed applications of deep UV LEDs include disinfection, sensing, water

* Project supported by the National High Technology Research and Development Program of China (No. 2013AA03A101).

† Corresponding author. Email: jmlj@semi.ac.cn

Received 16 May 2016

© 2016 Chinese Institute of Electronics

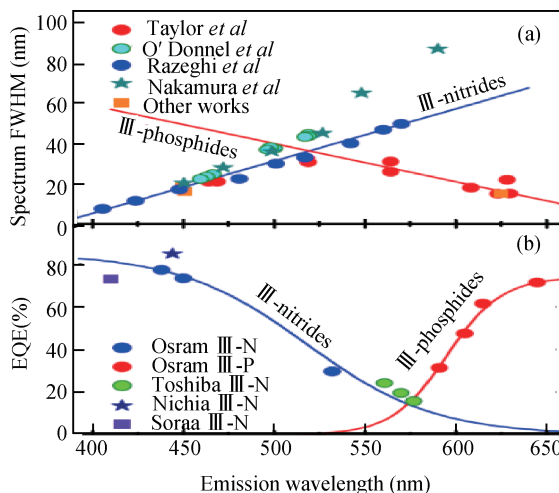


Figure 1. (Color online) (a) Spectrum FWHM and (b) maximum EQE of III-nitride and III-phosphide LEDs^[3].

purification, bio-medical, and communication. Improved material quality is key to achieving these aims.

Researchers in Institute of Semiconductors, CAS (IS-CAS) have been developing nano patterned-sapphire substrates (NPSS), achieved with nano-sphere lithography (NSL), as a basis for the production of superior aluminium gallium nitride (AlGaN) semiconductor material for deep UV LEDs. Sapphire patterning was achieved by photolithography through a mask consisting of polystyrene nanospheres that were then removed using deionized water (Figure 2). The pattern in the developed photoresist was transferred to an underlying hard mask layer of 200 nm silicon dioxide using inductively coupled plasma etch. Finally, the sapphire was wet etched using a mix of sulfuric and phosphoric acid solutions. The silicon dioxide was removed using hydrofluoric acid. The pattern consisted of 230-nm-deep concave triangular cones set in a hexagonal pattern of period 900 nm. The unetched region between the cones was 400 nm wide.

The growth of the UV LED epitaxial structure was through low-pressure metal-organic chemical vapor deposition (LP-MOCVD). The AlN was found to coalesce after only 3 μm . This is much sooner than other epitaxial layer overgrowth (ELOG) techniques using micro-stripe patterning that only coalesce after 10 μm growth. Atomic force microscopy (AFM) over $5 \times 5 \mu\text{m}^2$ fields gave a root-mean-square roughness of 0.15 nm. The AFM analysis also indicated a step-flow growth mode. X-ray analysis gave estimates for screw and edge dislocation densities of 1.6×10^7 and $1.2 \times 10^9 \text{ cm}^{-2}$, respectively.

This AlN template material was used in further growth of the UV LED structure. The same structure was grown on flat sapphire with a 1 μm AlN template layer. The n-AlGaN layer was found to have pure edge and mixed threading dislocation densities on NPSS and FSS substrates of $\sim 1.6 \times 10^9$ and $\sim 3.4 \times 10^9 \text{ cm}^{-2}$, respectively. The reduced density layer on NPSS was attributed to the higher-quality AlN template. The super-lattice regions were also designed to have dislocation filtering effects.

The epitaxial materials were formed into $380 \times 380 \mu\text{m}^2$ devices. The main electroluminescence (EL) peak occurred at

282 nm with a weak shoulder peak near 330 nm (Figure 3). Temperature-dependent photoluminescence studies at 10 and 300 K suggested an internal quantum efficiency of 45% for the NPSS LED structure, compared with 28% for the FSS AlN template epitaxy.

The light output power (LOP) at 20 mA current (I) was 3.03 mW with an external quantum efficiency (EQE) of 3.45% for the NPSS-based device. This was almost double that of the FSS-based LED. The saturation LOP for the NPSS LED was 6.56 mW at 60 mA current. The FSS device saturated at 2.53 mW with 50 mA injection.

2.2. Advanced heterostructure design

2.2.1. High efficiency multiple quantum well structure design

The large strain within the multiple quantum well (MQW) will result in the energy band of QWs being severely bended and the distributions of electrons and holes being separated towards opposite directions, leading to a strong quantum-confined stark effect (QCSE) and poor internal quantum efficiency (IQE)^[5, 6], as presented in Figure 4. Moreover, a high degree of carrier localization in green LEDs occurs due to inhomogeneous indium composition from differences in thermal dynamical and structural properties between GaN and InN, leading to carrier delocalization and overflow at high current^[7, 8]. The large strain and strong carrier localization within the active region are the major challenges in achieving high-efficiency green LEDs, which is referred to as a “green gap”^[9]. Recently, several specific structural designs have been proposed to alleviate the electrostatic field within MQWs and enhance the IQE of green LEDs, such as employing nonpolar and semipolar InGaN QWs^[10, 11], staggered InGaN QWs^[12–14], grade MQWs^[15], chirped MQWs^[16], InGaN-delta InN QWs^[17], and strain-compensated InGaN/GaN QW structure on InGaN substrates^[18].

Li^[19] has investigated InGaN-based green LEDs with low-indium-composition shallow quantum well (SQW) inserted before the InGaN emitting layer. Numerical simulation results show an increase of the overlap of electron-hole wave functions and a reduction of electrostatic field within the active region of the SQW LED, compared to those of the conventional LED, as shown in Figure 5. Photoluminescence (PL) measurements exhibit reduced full width at half maximum (FWHM) and increased PL intensity for the SQW LED. A 28.9% enhancement of output power at 150 mA for SQW LED chips of $256 \times 300 \mu\text{m}^2$ size is achieved.

Liu et al.^[20] have demonstrated the growth of quaternary AlInGaN compounds at different growth temperatures and pressures with metal organic chemical vapor deposition (MOCVD). The optical properties of the samples have been investigated by photoluminescence (PL) at different temperatures. The results show that the sample grown at a higher temperature (850 °C) exhibits the best optical quality for its sharp band edge luminescence and weak yellow luminescence. The AlInGaN exhibited a three-dimensional (3D) growth mode at the higher pressure. The band edge emission almost disappeared. With the optimization of AlInGaN growth parameters, we replaced the traditional barrier in InGaN/GaN MQWs with AlInGaN barriers. The peak wavelength for the

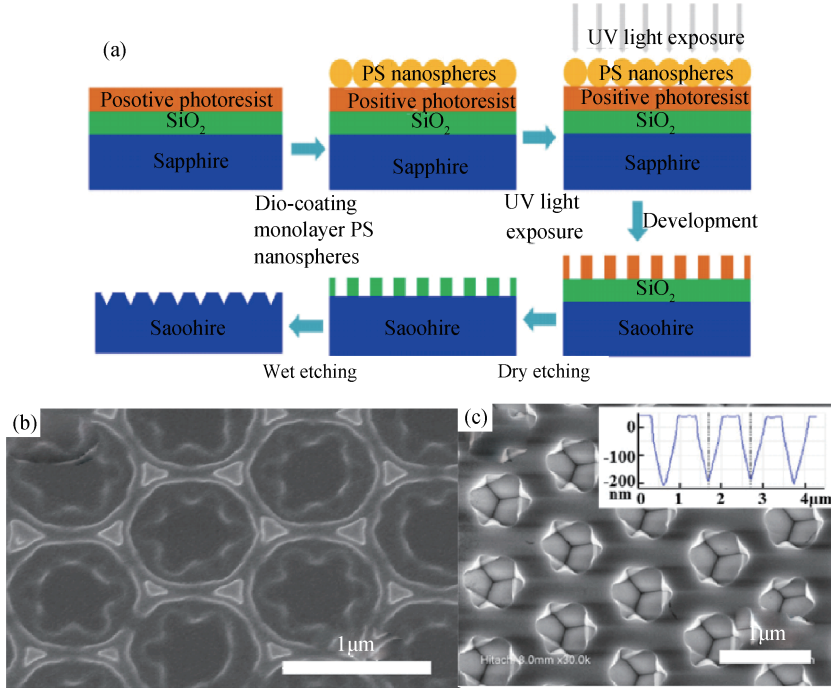


Figure 2. (Color online) (a) Schematic of fabrication process flow to create nano-patterns on a sapphire substrate (NPSS). SEM images of the (b) patterned photoresist and (c) wet-etched NPSS. Inset in Figure 2(c) shows line profile of patterns of NPSS by AFM measurement.

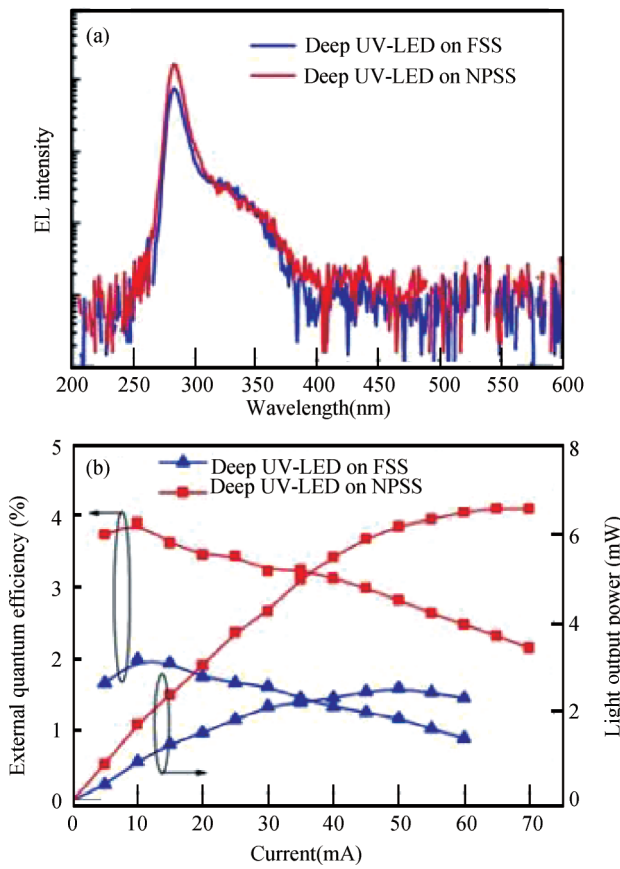


Figure 3. (Color online) (a) EL spectra and (b) LOP-I-EQE curves of deep UV LEDs grown on NPSS and FSS.

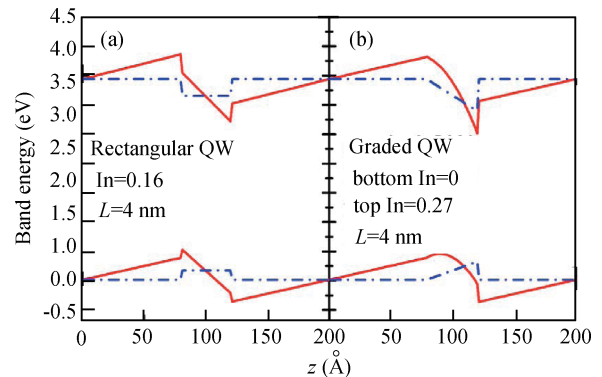


Figure 4. The energy band profiles of the C1 and the HH1 at Brillouin zone center for the ground state of conventional rectangular QW and graded QW with and without internal field^[15].

InGaN/AlInGaN-MQW based LEDs was very stable at various injection current levels because of the polarization-matched InGaN/AlInGaN MQWs, as illustrated in Figure 6.

2.2.2. Novel design for electron blocking layers

Insufficient electrons' blocking is still a big technical challenge for these devices to be competitive, especially for high-brightness applications^[21–23]. It is well known that in GaN-based devices the holes have a relatively high effective mass and hence a very low mobility making hole transport from the p-type layer to the active region difficult. This means electrons will then accumulate and recombine with holes at the top most quantum wells resulting in a relatively high local electron quasi-Fermi level, which increases the amount of electrons' overflowing across quantum barriers. A wide-band gap AlGaN layer called the electron blocking layer (EBL) is typ-

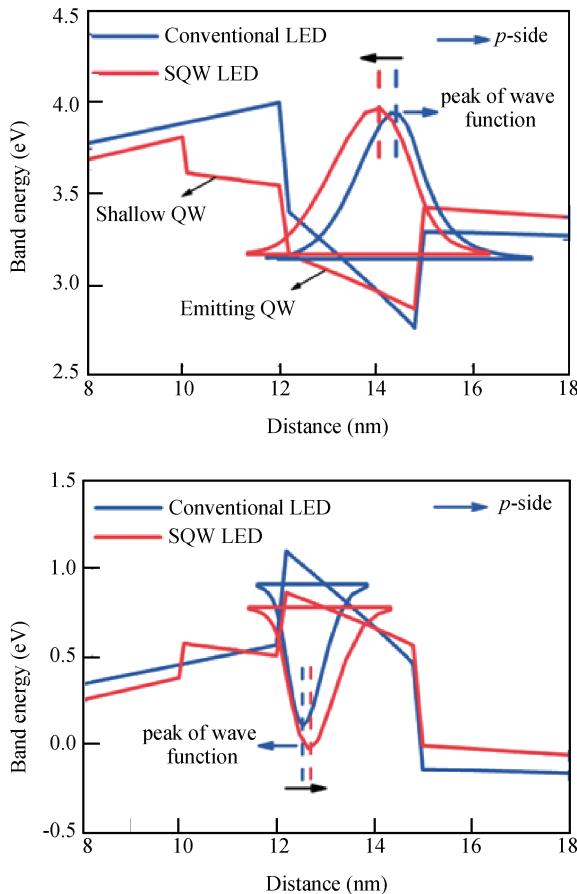


Figure 5. (Color online) Simulated energy band diagrams and electron–hole wave functions within the active region of the conventional LED and SQW LED^[19].

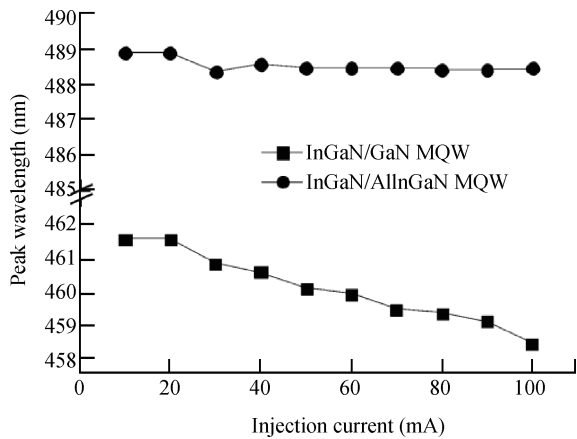


Figure 6. Peak wavelength of EL at different injection current levels in InGaN/GaN and InGaN/AlInGaN-MQW based LEDs^[20].

ically inserted between the active region and the p-type layer to prevent the electrons from overflowing out of the MQWs. However, the effectiveness of conventional EBLs in InGaN LEDs is still questionable. Recent research has shown that serious negative band-bending caused by the strong polarization at the last GaN barrier and the AlGaN EBL is present. As a result, the EBL that acts as a potential barrier for electrons fails in its original purpose. Furthermore, the AlGaN layer may also

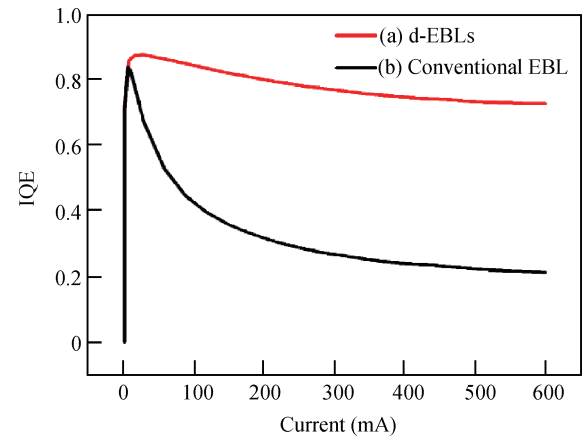


Figure 7. (Color online) The comparison IQE of (a) d-EBLs LED and (b) conventional LED.

act as both a potential barrier for electrons and holes depending on the band-offset ratio of the AlGaN/GaN hetero structure, thus reducing the hole injection efficiency as well as the quantum efficiency^[24–27]. Therefore, in order to enhance the hole injection without losing the electrons’ blocking capability, several alternatives of the AlGaN EBL have been explored and these include AlInGaN^[28], InAlN^[29, 30], graded Al profile AlGaN^[31, 32], and step graded AlGaN^[33].

Guo^[34] has proposed novel double electron blocking layers for InGaN/GaN multiple quantum wells light-emitting diodes to mitigate the efficiency droop at high current density. The band diagram and carriers distributions were investigated numerically. The results indicate that due to a newly formed holes stack in the p-GaN near the active region, the hole injection has been improved and a uniform carriers distribution can be achieved. As a result, in our new structure with double electron blocking layers, the efficiency droop has been reduced to 15.5% in comparison with 57.3% for the LED with AlGaN EBL at the current density of 100 A/cm², as shown in Figure 7.

Ren^[35] has proposed the InGaN/GaN green LED with a hybrid electron blocking layer (HEBL) formed by partially incorporating a small amount of indium in the AlGaN conventional electron blocking layer. The influence of the HEBL is investigated both experimentally and theoretically. By fitting the quantum efficiency with the modified ABCD model, these coefficients’ values are obtained and the reduced value of D suggests that the HEBL can weaken the carrier leakage. Subsequent simulation shows that the proposed design builds up two higher potential barriers for electrons and one lower potential barrier for holes, which could effectively enhance electron confinement and hole injection. Therefore, more carriers could be restricted in multiple quantum wells and participate in radiative recombination. As a result, the measured light output power of the proposed LED is 80% higher than that of the reference LED at a current of 150 mA and its external quantum efficiency droop ratio is also smaller.

Liu^[36] has studied the advantages of the p-InGaN/AlGaN electron blocking layer (EBL) for InGaN/GaN light-emitting diodes (LEDs) were studied numerically and experimentally. The LEDs with p-InGaN/AlGaN EBL exhibited better optical

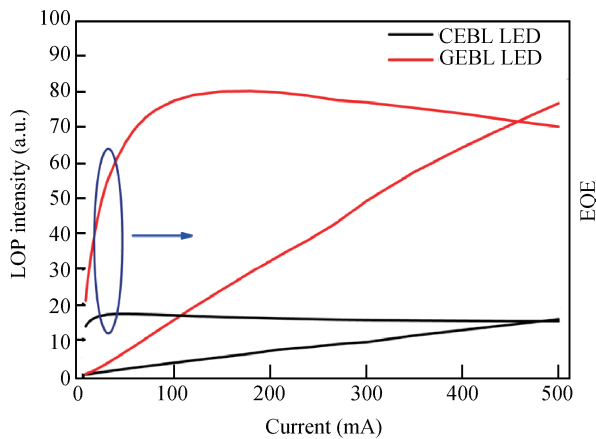


Figure 8. (Color online) LOP and EQE as a function of current for samples with a CEBL and a GEBL.

performance over a wide range of carrier concentrations due to the enhancement of holes' injection and electrons' confinement. The values of A, B, C, and D coefficients have been iteratively obtained by fitting quantum efficiency in the modified rate equation model. The analysis indicated that the improvement in the device properties could be attributed to the relatively small band gap and p-type doping of the InGaN insertion layer

Zhang^[37] has reported the effect of a graded AlGaN electron blocking layer (GEBL) on the emission properties of InGaN/GaN multiple quantum wells LED. The adoption of GEBL in the LED enhances the electroluminescence intensity and reduces the wavelength blue-shift with increasing injection current. The light output power of the GEBL LED is enhanced by 163% and 415% at 20 and 350 mA, respectively, which can be seen in Figure 8. Moreover, the forward voltage of the GEBLLED is reduced by 0.38V at the forward current of 20 mA.

2.3. High efficiency GaN based LEDs with extremely low thermal resistance

Recently, VLEDs was investigated extensively. Fabricated through the removal of insulating sapphire substrate and transferred to a new thermal and electrical conductive substrate, VLEDs have lower operation voltage, lower thermal resistance and higher saturation currents^[38–40], so it was undoubtedly considered to be the candidate for future high power and high efficiency LED devices.

Considering thermal dissipation, a method for manufacturing GaN based LEDs of the back hole structure was adopted. By introducing the back hole technique into the silicon based microelectronics processes to this method, the silicon oxide insulation layer in the heat conducting path can be removed, and the silicon is replaced by the copper, whose heat conductivity is almost 3 times that of the silicon, thus enabling the heat produced in the active region of the LED die to be directly conducted to the heat sink through the metal, which is an excellent heat conductor, and the whole heat dissipation path includes no poor heat conductor, thus reducing the thermal resistance as much as possible, and realizing the heat dissipation with a so-called sub-zero thermal resistance. This method not only makes

the LEDs able to work at a larger operating current, but also improves their ability to work continuously for a long time, which enhances the performance and reliability, thus facilitating the realization of the power LED for illumination.

Ni/Ag based metal layers were used as p contact, which has high reflectivity in the visible light region. The p type ohmic contact resistance was brought down by optimized p GaN growth conditions and p metal annealing. To reduce the n type ohmic contact resistances, a new scheme for depositing metallization contacts has been developed. This includes chemical cleaning, selectively wet etch surface roughing, and Al based multi metal layers were deposited on the n type GaN. Chemical cleaning is effective to reduce the contact resistance.

Based on those methods, VLEDs were fabricated, which show extremely high peak efficiency (>200 lm/W), low operating voltage (2.75 V @ 350 mA), low reverse leakage current (0.015 μ A @ -5 V), low thermal resistance (2.5 K/W) and high saturation currents. The saturation current is beyond 4 A.

2.4. Progress on p-doping of GaN

GaN-based light emitting diodes (LEDs) are suffering from a low hole injection efficiency because of the inefficient p-doping in the wide-band gap nitrides^[41, 42]. This problem emerging since the early 1990s is becoming increasingly troublesome for high power LEDs^[43, 44]. Several methods have been performed to attempt to achieve a high hole concentration through raising the activation efficiency of Mg, which include low-energy electron-beam irradiation treatment^[45], thermal annealing^[46], and metal catalytic treatment^[47].

2.4.1. Polarization induced 3D hole gas

P-type conductivity is always a difficult technique for wide-band-gap III-nitride semiconductor materials. In 2010, a p-type doping method named polarization-doping was proposed by Simon in the N-face graded AlGaN layer. However, N-face GaN-based structures tend to have poor surface morphology and high impurity concentration, no matter whether they are grown by MOCVD or molecular beam epitaxy^[48]. Researchers at ISCAS achieved three-dimensional hole gas (3DHG) in (0001)-oriented graded AlGaN by using polarization-doping. The hole concentration in the graded AlGaN layer is as high as $\sim 10^{18}$ cm⁻³ at RT and shows weak temperature dependence^[49].

The metal-face graded AlGaN is grown by single-wafer home-made MOCVD. Before growing the graded AlGaN layer, a 1 μ m thick un-doped AlN layer is deposited on the c-plane sapphire at 1200 °C. Then a 100 nm thick Mg-doped graded Al_xGa_{1-x}N layer with Al composition from $x = 0.3$ to 0 is grown on the AlN layer.

For the metal-face graded AlGaN layer grown on the AlN layer, N unit cells with an Al composition are linearly decreasing from $x = 0.3$ to 0. The unbalance bound sheet charge density is Al composition dependent, which decreases as the Al composition decreases, as shown in Figure 9. The net bound sheet charge density at the interface of the i th and $(i+1)$ th unit cell is then summed as $[(P_i^{\text{sp}} + P_i^{\text{pe}}) - (P_{i+1}^{\text{sp}} + P_{i+1}^{\text{pe}})]/q$. $P_i^{\text{sp}} - P_{i+1}^{\text{sp}} < 0$, and $P_i^{\text{pe}} - P_{i+1}^{\text{pe}} < 0$, meaning that the net bound sheet charges are negative at the interface of each unit cell. Consequently, equivalent holes at the interface of each

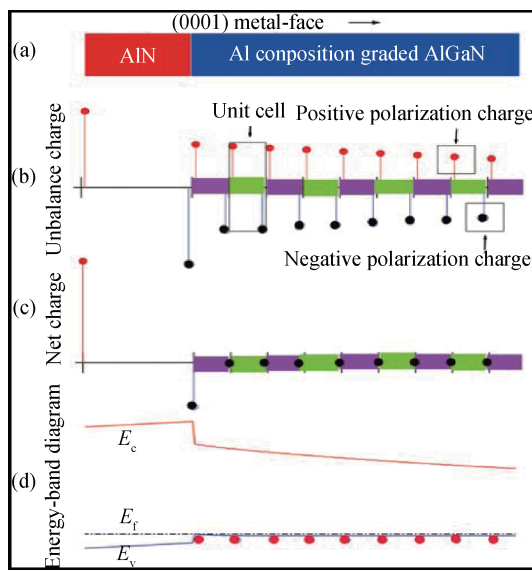


Figure 9. (Color online) Schematic illustration of polarization-induced 3DHG in (0001)-oriented metal-face III-nitride structure.

unit cell are induced from the acceptors (Mg) by the polarization field to neutralize the negative bound sheet charges. These holes spread over the graded AlGaN layer continuously, thus forming a mobile 3DHG.

The RT hole concentration of the graded AlGaN layer is $2.6 \times 10^{18} \text{ cm}^{-3}$, one order of magnitude higher than that of the GaN layer ($2.5 \times 10^{17} \text{ cm}^{-3}$). As the temperature decreases, the hole concentration of the GaN layer drops exponentially caused by carrier freeze out due to the high activation energy of Mg in GaN, as shown in Figure 10. While for the graded AlGaN layer, the hole concentration shows weak temperature dependence, it is as high as $4.5 \times 10^{17} \text{ cm}^{-3}$ when the temperature is down to 100 K. This reveals that the holes in the graded AlGaN layer are induced by polarization, because the polarization-doping does not need thermal ionization energy to activate it. The RT resistivity of the graded AlGaN layer is $0.6 \Omega\cdot\text{cm}$, lower than that of the GaN layer ($1.8 \Omega\cdot\text{cm}$), indicating an enhanced p-type conductivity in the graded AlGaN layer. Besides, as the temperature decreases, the resistivity of the graded AlGaN layer increases slower than that of the GaN layer^[50].

2.4.2. Impurity resonant state p-type doping

A novel strategy for efficient p-type doping was proposed to overcome the fundamental problem of high activation energy in high bandgap III-nitrides by introducing impurity resonant states in an Mg doped $\text{Al}_x\text{Ga}_{1-x}\text{N}/\text{GaN}$ superlattice structure. The characteristics and distribution of Mg impurity states were analyzed using first-principle calculations. The results, as Figure 11 shows, indicated that the coupling and hybridization between Mg 2p impurity states and N 2p states is likely to be the main reason for the delocalized characteristics of the Mg impurity states. As a result, the wave-functions of Mg impurity states in the barrier layers are able to overlap with each other, then extended into well layers and act as resonant states. Therefore, a high hole concentration (about one order of magnitude higher than normal bulk Mg doped nitrides) could be success-

fully realized. This structure can be used to achieve efficient nitride based optoelectronic devices, especially in the deep ultraviolet wavelength range. The concept of impurity resonant state p-type doping presented here could also be applied to the production of highly p-type conductors in other wide-bandgap materials. The optimization on the thickness and components of $\text{Al}_x\text{Ga}_{1-x}\text{N}/\text{GaN}$ structures is highly desired to obtain higher hole concentrations, as will be investigated in the subsequent works. Finally, the two-carrier-species Hall-effect model was used to extract the electrical parameters of bulk holes and 2D hole gases in superlattice-like structures, respectively. The model reported here can also be used to explain the abnormal and seldom analyzed freeze-in effect observed in many previous reports^[51].

2.4.3. Co-doping for effective p-doping

Recently, another effective strategy for achieving efficient p-type doping in wide bandgap nitride semiconductors was proposed to overcome the fundamental issue of the high activation energy by Liu *et al.*^[52]. They demonstrate that a hole concentration as high as $1.4 \times 10^{18} \text{ cm}^{-3}$ could be achieved through In–Mg Co-doping. The electronic structure of the system and the formation energy of impurity are analyzed via first principle calculation to clarify the underlying physics and the ambiguity in understanding of the origin of the high hole concentration, which is presented in Figure 12. The results indicate that the original valence band maximum of the host materials could be modified, thus improving the p-type doping ability and the calculated ionization energy of the acceptor is only about 135 meV, which is much smaller than that of the isolated Mg acceptor.

2.5. Edge-cutting technology for GaN LEDs

2.5.1. Nanostructure LED

Recently, the nanowire LED^[53–57], mainly a core/shell LED, has attracted a large amount of attention because of their potential advantages. In comparison to the conventional thin film LEDs, core/shell nanorod structure LEDs have a higher aspect ratio and larger active regions. Besides, the InGaN/GaN multi-quantum wells (MQWs) grown on nonpolar or semipolar GaN facets are suggested to be able to effectively increase the light extraction efficiency and reduce the quantum confined Stark effect (QCSE), which increases the internal quantum efficiency of LEDs through enhancing the radiative recombination rate in MQWs^[58–60]. What is more, nitride nanowires could improve the material quality with respect to thin films, which better handle the strain induced by the thermal expansion mismatch.

For the structure of core/shell LED, the growth of high density ordered GaN nanowires (core) is necessary for the follow-up metal contacting and homogeneous radial growth. The top-down etching and bottom-up selective area MOCVD growth^[61, 62] are two prevailing GaN nanowire growth methods. We have widely studied these two methods^[63–68]. GaN dry plasma etching is widely used in the III nitrides industry. However, reactive ion etching (RIE) suffers from relatively low etch rates and plasma damage in devices. Compared with RIE, wet-etching has the advantages of reducing surface damage and low cost, and providing a simple method for device

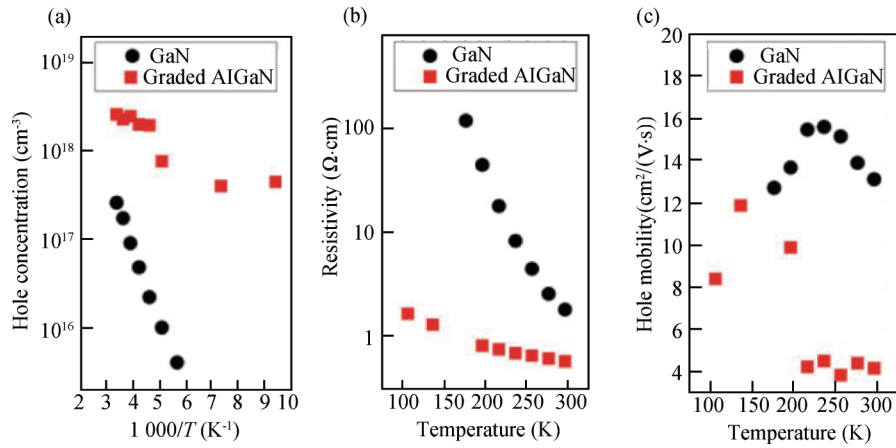


Figure 10. (Color online) Temperature-dependent Hall-effect measurements for the GaN layer and the graded AlGaN layer.

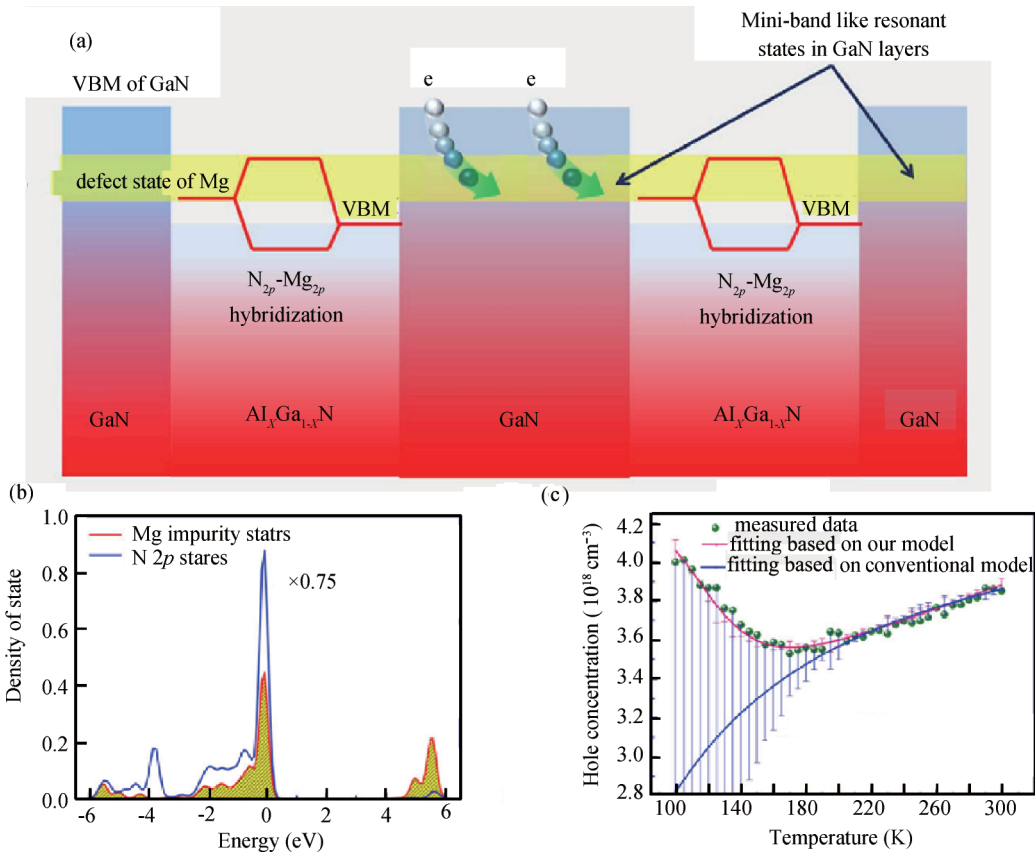


Figure 11. (Color online) (a) Schematic model showing the mechanism of impurity resonant states p-type doping. (b) Evidence for the de-localization characteristics of Mg impurity states. Calculated projected density of states of Mg 2p impurity states and N 2p states. (c) Hole concentration as a function of temperature. The fitting curves are shown as solid lines using a conventional Hall-effect model and a two-carrier-species Hall-effect model.

fabrication. Figure 13 shows the nanostructure mainly developed by wet etching. We found the suppression of the etch rate in the vertical direction could help to form the uniform nanowire. A thin AlGaN which was stable in the KOH solution was used to suppress the vertical direction. The wetting nanowires were surrounded by six $\{1\bar{1}00\}$ m planes. On the other hand, the existing large vertical etching could develop the pyramid structure with six $\{11\bar{2}1\}$ facets. The top-down approach may be an effective method to obtain the array

nanowires. However, the nanowire crystal quality was poor because of the film growth and wetting. The selective area growth (SAG) was the most effective GaN nanowire growth method because of the high crystal quality and there being no introduction of foreign metals. Our team also systematically studied the growth technology. We found the hydrogen content has a large impact on the morphology of the nanostructure. Interestingly, the results were similar to the wet etching. The high hydrogen content benefited from the development of long one-

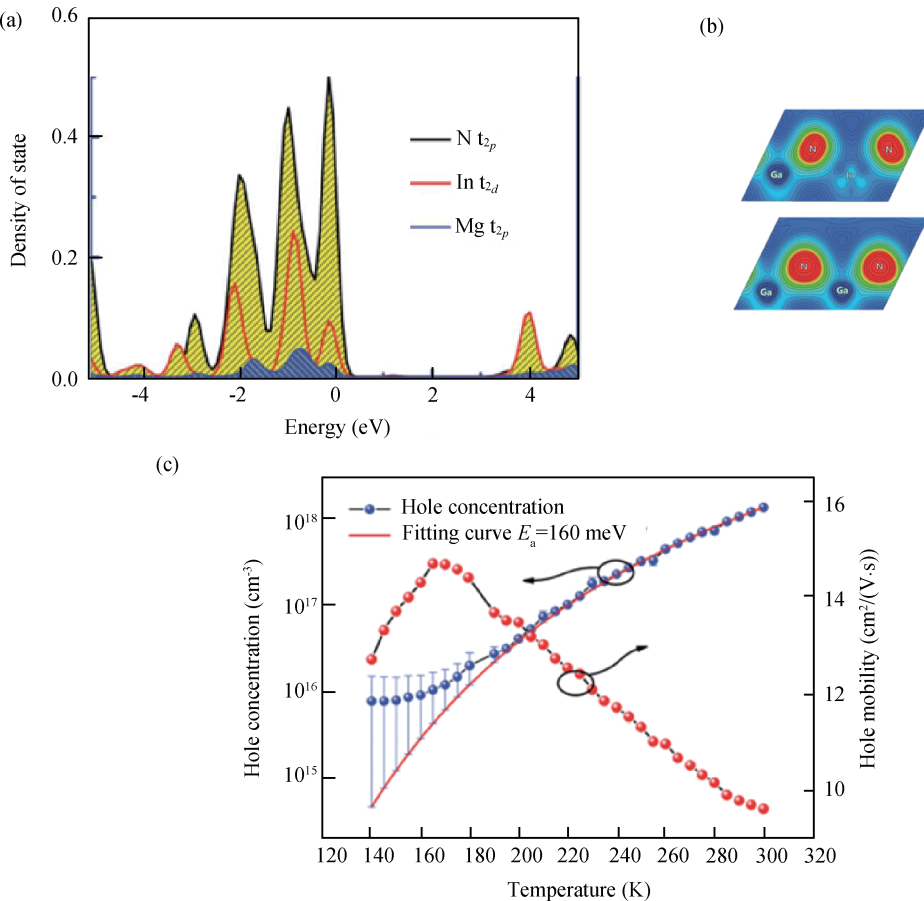


Figure 12. (Color online) (a) Calculated projected density of state of In 4d, N 2p and Mg 2p orbital. (b) Isosurface charge density plots of VBM of In-Mg co-doping GaN at the G point in the planes of N-In-N bonds and N-Ga-N bonds. (c) Hole concentration and mobility as a function of temperature for In-Mg co-doped GaN samples. The fitting curve is shown with a solid line.

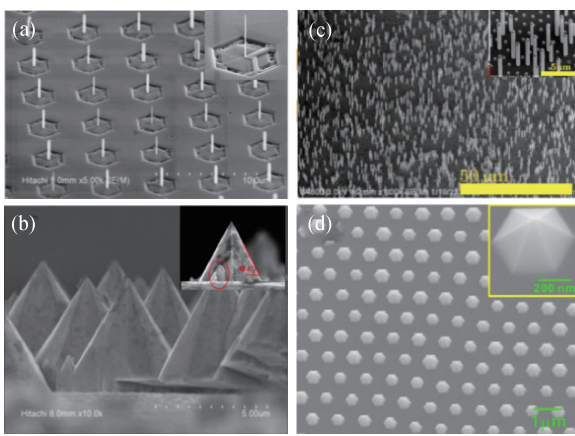


Figure 13. (Color online) The development of GaN nanostructure by wet etching (a and b) and selective area growth (c and d): (a) wet etching with a thin AlGaN cap^[65], (b) wet etching without a thin AlGaN cap^[64], (c) selective area growth with high hydrogen content^[66], and (d) selective area growth with high hydrogen content^[67].

dimensional nanorods while a lack or no hydrogen carrier gas lead to the formation of the pyramid structure. The morphology change of GaN nanostructures with H₂ flow rate could be explained by the two functions of hydrogen, that is, the passivation and etching effects, during the growth process. The

semipolar $\{1\bar{1}01\}$ *r*-plane is an N-terminated surface, which is easily passivated by the hydrogen atoms from NH₃ or H₂. Thus, the low hydrogen content could benefit the *r*-plane. However with increasing the H₂ flow rate, the etching effect of H₂ starts to dominate. Consequently some pyramids are etched and the *m*-plane is exposed, which leads to the presence of nanorods.

The high current driven, high brightness InGaN/GaN core-shell LED is the final aim for our study. Figure 14 shows the pyramid array InGaN/GaN core-shell light-emitting diodes (LEDs) which were fabricated by using a highly homogeneous multilayer graphene transparent conducting electrode. The key fabrication procedures are the SAG growth of the pyramid n-doped GaN, low temperature P-GaN growth, translating graphene acted as the p-type electrode and depositing the p- and n-GaN contact pads. The EL spectra [Figure 14(c)] of graphene interconnect pyramid array core-shell LEDs exhibits a dominant emission peak at 478 nm with no noticeable spectral shift as the injection current is increased from 2 to 90 mA. This result is attributed to the fact that the built-in strain in the MQWs is very small in these pyramid array InGaN/GaN core-shell LEDs and the piezoelectric field also decreases effectively by growing MQWs on a semipolar facet ($1\bar{1}01$) GaN pyramid sidewall. The current-voltage (*I*-*V*) curve shows rectifying characteristics with a dynamic resistance at various current. The dynamic resistance originates from the contact resistance of p-GaN and graphene. The reversed leakage current of pyramid array core-

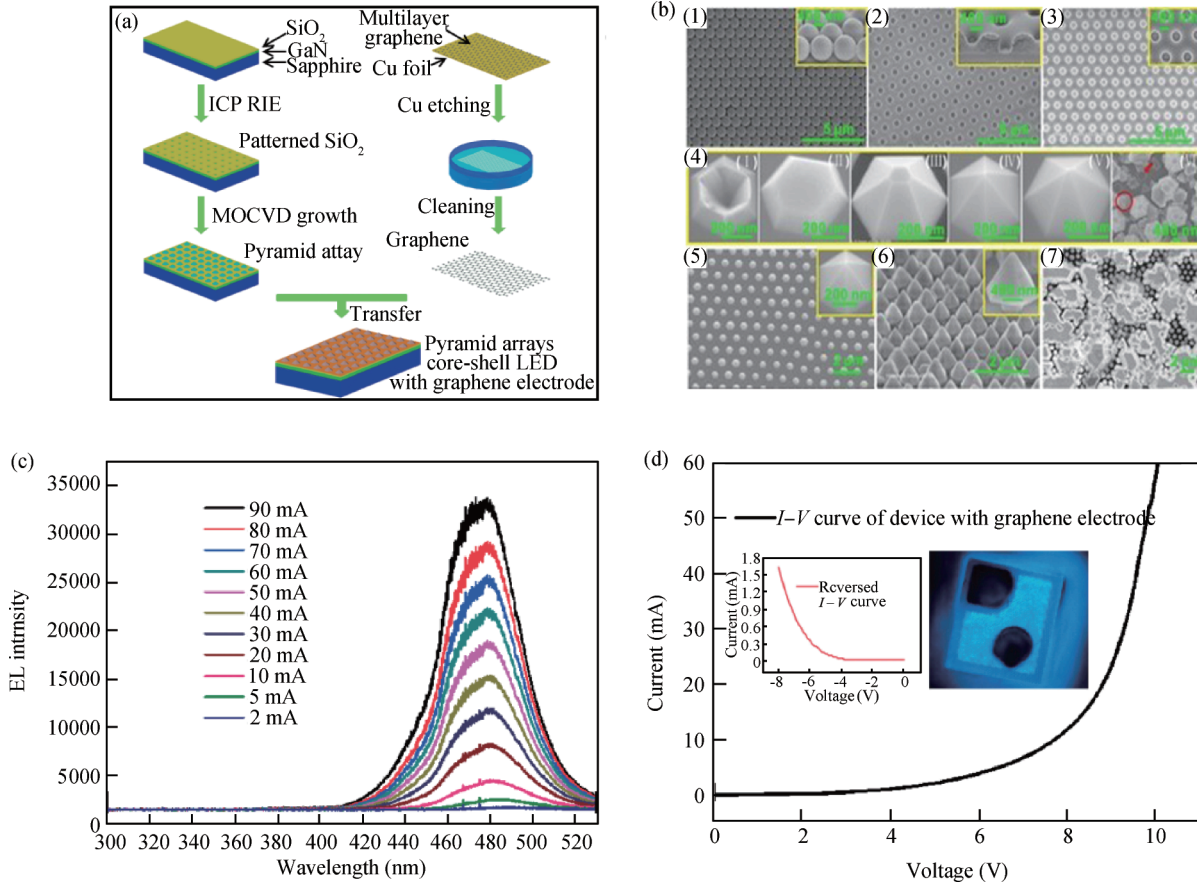


Figure 14. (Color online) Pyramid array core-shell LED with graphene electrodes. (a) Schematic illustration of the key fabrication procedures (b) SEM image of large-area pyramid core-shell LED fabrication procedures. (c) Room-temperature EL spectra of pyramid array core-shell LED at various current injections. (d) I - V curve of LEDs with multilayer graphene electrode. The inset is a photograph of the light emission from a single LED chip and reversed bias voltage I - V curve^[67, 68].

shell LEDs is about $1.6 \mu\text{A}$ @ 8 V [inset of Figure 14(d)], which indicates that the device has good reliability. The illumination photo [inset of Figure 14(d)] of the LED chip at 20 mA shows uniform luminosity, which indicates the good current spreading by using graphene electrodes.

2.5.2. 2D graphene

Attributed to its significant electrical, optical, mechanical, and chemical properties, graphene is expected to play an important role in future uses as a functional component in electronic and optoelectronic devices, such as transistors, integrated circuits, solar cells, and LEDs^[69]. Graphene can work as transparent conductive electrodes in LEDs, which has been widely demonstrated, and it can also work as a buffer layer. In this part, we will mainly focus on these two usages of graphene.

(a) Graphene as transparent conductive electrodes (TCEs)

Graphene is a promising next-generation conducting material with the potential to replace traditional electrode materials such as indium tin oxide (ITO) in electrical and optical devices. Conventional ITO TCEs are widely used in GaN-based LEDs. It has a low sheet resistance of less than 100Ω , high optical transparency of ~90%, and unlimited scalability. However, ITO is also criticized for its high cost due to the rarity of the indium elements, poor transparency in the near ultravi-

olet and ultraviolet ranges, instability in the presence of acids or alkalis, and susceptibility to ion diffusion into the substrate. Moreover, ITO is fragile and cannot withstand the high temperature procedures^[70].

Currently, to solve these problems, new types of transparent conductive electrodes are extensively investigated, including conducting oxides^[71], metals^[72], carbon nanotubes^[73], and graphene^[74]. Among these novel transparent conductive electrodes, graphene is considered to be an ideal candidate to replace traditional ITO electrodes because of its outstanding electrical [with reported electron mobility values in excess of $15\,000 \text{ cm}^2/(\text{V}\cdot\text{s})$], optical (with 97.7% transmittance for single layer graphene), thermal [with near-room temperature thermal conductivity between $(4.84 \pm 0.44) \times 10^3$ and $(5.30 \pm 0.48) \times 10^3 \text{ W}/(\text{m}\cdot\text{K})$] mechanical and chemical properties. Based on such considerations, graphene films have been used in GaN-based LEDs and ultraviolet LEDs as transparent electrodes.

Schematics of the G-LED fabrication process are illustrated in Figures 15(a)–15(d). First, the graphene film was transferred onto the p-GaN layer. Then, the LED mesa was obtained by standard lithography patterning followed by applying an inductively coupled plasma (ICP) etcher using Cl₂ and BC_l₃ to expose the n-type GaN layer. Finally, the p- and n-electrodes composed of Cr/Au were evaporated onto the graphene layer and the n-type GaN layer by e-beam evaporating.

However, it should be noted that we cannot obtain CVD-

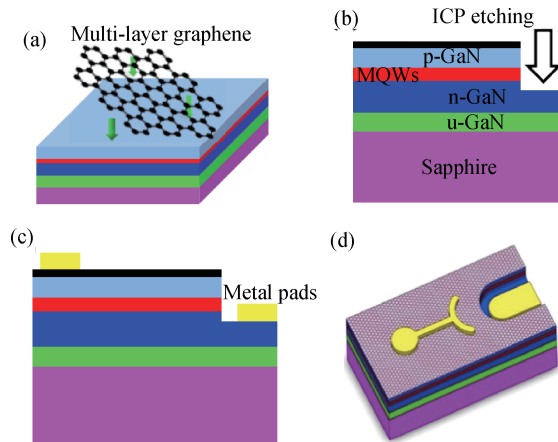


Figure 15. (Color online) (a)–(c) Schematics of the G-LED fabrication process. (d) Structure of a G-LED.

grown graphene of high quality and large areas. Defects (such as dislocation, steps and grain boundaries) formed during epitaxial growth and disruptions (such as wrinkles, cracks and edges) formed during the transfer process, can effectively scatter the charge carrier, leading to the degradation of the transport properties of graphene and higher electrical resistivity. In addition, due to the high work function mismatch between p-, n-GaN and graphene, it is hard to achieve low contact resistance for both p-, n-GaN/graphene hetero junctions, especially for p-GaN with lower carrier concentration. GaN/graphene heterojunction barriers will hinder the movement of carriers, increase the forward operating voltage of LEDs, and weaken the advantage of graphene as a transparent current spreading layer. We have adopted several methods to alleviate these problems, such as annealing, nitric acid doping, and hybrid electrode.

Annealing. Zhang *et al.*^[75] fabricated InGaN green LEDs (GLEDs) with multiple-layer graphene (MLG) electrodes and examined the $I-V$ characteristics of the annealed MLG-GLEDs. It was found that the light-emitting performance of MLG-GLEDs could be improved with appropriate annealing. Wang *et al.*^[76] proved it using the CTLM method. He found that the resistance for the graphene/GaN contact is determined mainly by the work function gap and the carrier concentration in GaN, the polarity and the process-induced material variation; further annealing causes the metal atoms to diffuse across graphene and directly contact with the underlying GaN layer.

Nitric acid doping. The electrical characteristics of GaN/graphene junctions can be improved by nitric acid doping. It was found that HNO_3 doping can significantly increase the junction conductance, which is advantageous for LEDs to reduce the operating voltage. Chip test results of the vertical structure LEDs (VLEDs) confirm this acid induced improvement in forward electrical characteristics and light output power^[77]. The results can be seen in Figure 16.

Hybrid electrode. Li *et al.*^[78] introduced Ag nanowires (AgNWs) below the graphene films to improve the electrical conductivities and decrease the sheet resistance of graphene. It was found that the graphene/AgNWs hybrid films exhibited high transmittance and lower sheet resistance compared to bare graphene. The specific contact resistance between graphene and p-GaN reduced nearly by one order of magnitude with the introduction of AgNWs. The enhanced performance was at-

tributed to the bridging by AgNWs of cracks, grain boundaries in graphene and the reduction of the Schottky barrier height at the graphene/p-GaN interface. The schematics and results were shown in Figure 17.

Zhang *et al.*^[79] adopted a NiO_x buffer layer to improve its ohmic contact with the underlying p-GaN layer. They demonstrated that the large work function of the NiO_x interlayer reduces the contact barrier at the graphene/p-GaN layer interface. Moreover, the high p-type carrier concentration of NiO_x caused by the nickel vacancies and/or oxygen interstitials makes it easier for graphene to form ohmic contacts with the p-GaN layer and consequently improves the LED performance.

Using graphene TCEs, we have also obtained several devices, such as GaN-based nanorod LEDs^[80] phosphor-free InGaN micro-pyramid white LEDs^[81], monolithic integration of GaN-based LEDs^[82] and so on.

(b) Graphene as the buffer layer

The common GaN growth method is heteroepitaxial growth, which has strong chemical bonds at the interface to connect the epilayer and the substrate, so that it intensely depends on the match between the substrate and the epilayer. The heteroepitaxial substrate (Si, sapphire, SiC) can bring many defects and dislocation during the epitaxial process because of the mismatch, so the quality of the GaN films is reduced. Recently, another growth mechanism was reported to improve the heteroepitaxial growth of GaN. That is van der Waals epitaxy (vdWE)^[83], which means the connections between the substrate and the epilayer are weak van der Waals interactions rather than strong chemical bonds, so we can ignore the mismatch in this way.

In vdWE, the nucleation is the main aspect we should focus on, due to the lack of dangling bonds. At the beginning, other nucleation layers were used to increase the nucleation sites, such as ZnO ^[84], and AlN ^[85], however, the result was not as good as expected. Then the experiment of GaN growth without other nucleation layers were carried out. Kim *et al.*^[86] adopted the graphene produced by thermal decomposition of SiC and the formed steps to promote the GaN growth. The film was found to be of high quality, whose RMS was only 3 Å, and the full-width half maximum (FWHM) of the GaN (0002) peak was 0.06°. Balushki *et al.*^[87] demonstrated the im-

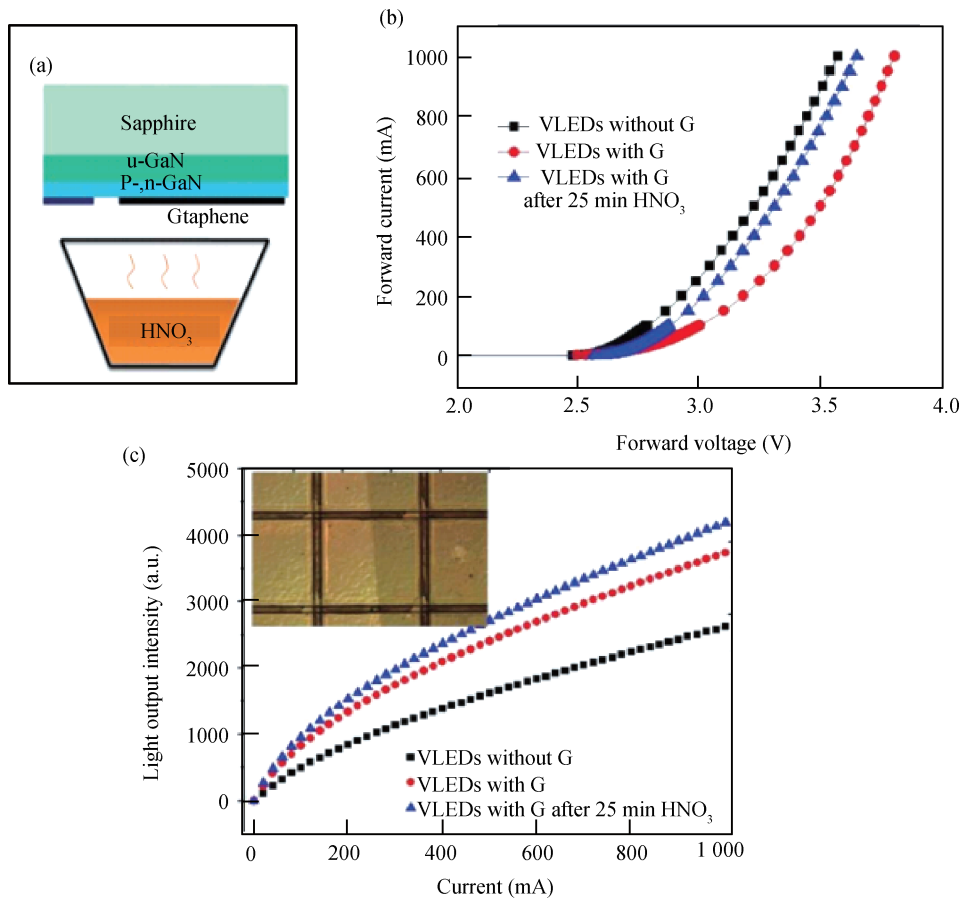


Figure 16. (Color online) (a) Schematics of the nitric acid doping process. (b) Forward I - V curves of VLEDs before and after acid doping. (c) Light output power of VLEDs versus different forward current.

pact of graphene properties on GaN and AlN nucleation using this method. It was found that the nucleation of AlN and GaN was along the periodic EG coated step edges rather than the terraces, and it preferred the defects sites. Also, the increased temperature can promote the growth of the nucleation. Chae *et al.*^[88] treated graphene with oxygen to increase the defects sites to promote the nucleation, and they obtained high-quality GaN film without a yellow luminescence band.

Our group also planned to study the vdWE growth of GaN film. We grew the GaN film on transferred-graphene/sapphire substrate. The graphene was grown on copper foil and then transferred to the substrate, then the growth was carried out at 1045 °C. The SEM result is shown in Figure 18. It shows that the GaN films with graphene are flatter and own a larger crystalline grain. We also tested the RMS of both samples, which shows that the RMS reduced from 21 to 0.8 nm because of the introduction of graphene. However, the XRD result was not so good. The FWHM of the samples with graphene is 928.4 arcsec, which is still high despite a 167 arcsec reduction compared to the sample without graphene.

3. Conclusion

In this paper, we present some of our recent research on the materials physics, crystal growth, device physics and advanced heterostructure design. A serious solution for high efficiency LEDs with extremely low thermal resistance was

demonstrated. We believe that solid-state-lighting technology is presently going through a revolution, namely the transition from light bulbs and fluorescent tubes to LEDs; it will continue to change our life in many ways.

References

- [1] The Royal Swedish Academy of Sciences. Scientific background on the Nobel prize in physics 2014: efficient blue light-emitting diodes leading to bright and energy-saving white light sources, 2014
- [2] Cho J, Schubert E F, Kim J K. Efficiency droop in light-emitting diodes: challenges and countermeasures. *Laser & Photonics Reviews*, 2013, 7: 408
- [3] Bulashevich K A, Kulik A V, Yu S, et al. Optimal ways of color mixing for high-quality, white-light LED sources. *Phys Status Solidi A*, 2015, 212: 914
- [4] Dong Peng, Yan Jianchang, Wang Junxi, et al. 282-nm AlGaN-based deep ultraviolet light-emitting diodes with improved performance on nano-patterned sapphire substrates. *Appl Phys Lett*, 2013, 102(24): 241113
- [5] Ryou J H, Yoder P D, Liu J P, et al. Control of quantum-confined stark effect in InGaN-based quantum wells. *IEEE J Quantum Electron*, 2009, 15: 1080
- [6] Park S H, Ahn D, Kim J W. High-efficiency staggered 530 nm InGaN/InGaN/GaN quantum-well light-emitting diodes. *Appl Phys Lett*, 2009, 94: 041109
- [7] Wang J X, Wang L, Zhao W, et al. Understanding efficiency droop effect in InGaN/GaN multiple-quantum-well blue light-

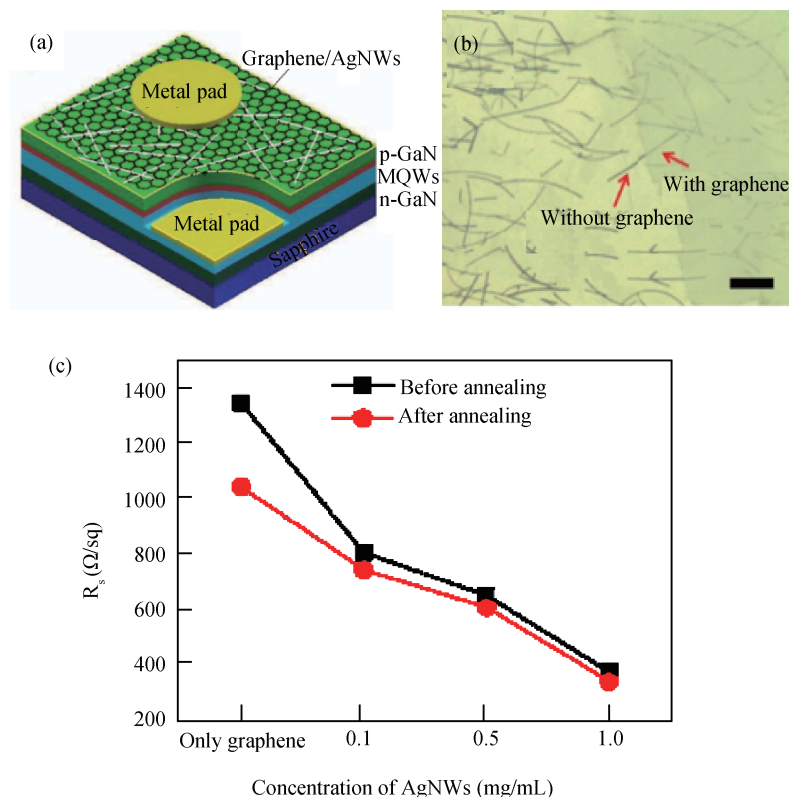


Figure 17. (Color online) (a) Schematic diagram of an LED device with graphene/AgNWs hybrid film. (b) Optical image of graphene/AgNWs hybrid film. (c) Light output power of VLEDs versus different forward current. Sheet resistances of bare graphene and graphene/AgNWs hybrid films before and after thermal annealing.

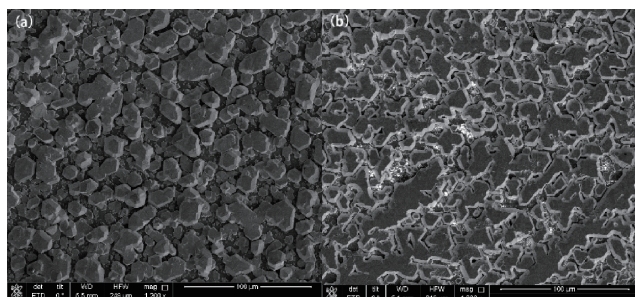


Figure 18. (Color online) SEM of GaN films (a) without graphene buffer, and (b) with graphene buffer.

- emitting diodes with different degree of carrier localization. Appl Phys Lett, 2010, 97: 201112
- [8] Shin D S, Han D P, Oh J Y, et al. Understanding efficiency droop effect in InGaN/GaN multiple-quantum-well blue light-emitting diodes with different degree of carrier localization. Appl Phys Lett, 2012, 100: 153506
- [9] Park I K, Park S J. Green gap spectral range light-emitting diodes with self-assembled InGaN quantum dots formed by enhanced phase separation. Appl Phys Express, 2011, 4: 042102
- [10] Farrell R M, Feezell D F, Schmidt M C, et al. Continuous-wave operation of AlGaN-cladding-free nonpolar *m*-plane InGaN/GaN laser diodes. Jpn J Appl Phys, 2007, 46: L761
- [11] Sharma R, Pattison P M, Masui H, et al. Demonstration of a semipolar (10̄13) InGaN/GaN green light emitting diode. Appl Phys Lett, 2005, 87: 231110
- [12] Arif R A, Ee Y K, Tansu N. Polarization engineering via staggered InGaN quantum wells for radiative efficiency enhancement

- of light emitting diodes. Appl Phys Lett, 2007, 91: 091110
- [13] Arif R A, Zhao H, Tansu N. Type-II InGaN–GaNAs quantum wells for lasers applications. Appl Phys Lett, 2008, 92: 011104
- [14] Zhao H, Liu G, Li X, et al. Growths of staggered InGaN quantum wells light-emitting diodes emitting at 520–525 nm employing graded growth-temperature profile. Appl Phys Lett, 2009, 95: 061104
- [15] Wang L, Li R, Yang Z, et al. High spontaneous emission rate asymmetrically graded 480 nm InGaN/GaN quantum well light-emitting diodes. Appl Phys Lett, 2009, 95: 211104
- [16] Chang Y A, Kuo Y T, Chang J Y, et al. Investigation of InGaN green light-emitting diodes with chirped multiple quantum well structures. Opt Lett, 2012, 37: 2205
- [17] Zhao H, Liu G Y, Tansu N. Analysis of InGaN-delta-InN quantum wells for light-emitting diodes. Appl Phys Lett, 2010, 97: 131114
- [18] Zhang J, Tansu N. Improvement in spontaneous emission rates for InGaN quantum wells on ternary InGaN substrate for light-emitting diodes. J Appl Phys, 2011, 110: 113110
- [19] Li Hongjian, Li Panpan, Kang Junjie, et al. Quantum efficiency enhancement of 530 nm InGaN green light-emitting diodes with shallow quantum well. Appl Phys Express, 2013, 6: 052102
- [20] Liu Naixin, Wang Junxi, Yan Jianchang, et al. Characterization of quaternary AlInGaN epilayers and polarization-reduced InGaN/AlInGaN MQW grown by MOCVD. Journal of Semiconductors, 2009, 30: 113003
- [21] Nakamura S. The roles of structural imperfections in InGaN-based blue light-emitting diodes and laser diodes. Science, 1998, 281: 956
- [22] Schubert E F, Kim J K. Solid-state light sources getting smart. Science, 2005, 308: 1274
- [23] Han S H, Lee D Y, Lee S J, et al. Effect of electron blocking

- layer on efficiency droop in InGaN/GaN multiple quantum well light-emitting diodes. *Appl Phys Lett*, 2009, 94: 231123
- [24] Lee J, Li X, Ni X, et al. On carrier spillover in *c*-and *m*-plane InGaN light emitting diodes. *Appl Phys Lett*, 2009, 95: 2011135
- [25] Yen S H, Tsai M C, Tsai M L, et al. Effect of n-type AlGaN layer on carrier transportation and efficiency droop of blue InGaN light-emitting diodes. *IEEE Photonics Technol Lett*, 2009, 21: 975
- [26] Schubert M F, Xu J, Kim J K, et al. Polarization-matched GaInN/AlGaN multi-quantum-well light-emitting diodes with reduced efficiency droop. *Appl Phys Lett*, 2008, 93: 041102
- [27] Min-Ho K, Schubert M F, Qi D, et al. Origin of efficiency droop in GaN-based light-emitting diodes. *Appl Phys Lett*, 2007, 91: 183507
- [28] Kuo Y K, Tsai M C, Yen S H. Numerical simulation of blue InGaN light-emitting diodes with polarization-matched AlGaN electron-blocking layer and barrier layer. *Opt Commun*, 2009, 282: 4252
- [29] Kim H J, Choi S, Kim S S, et al. Improvement of quantum efficiency by employing active-layer-friendly lattice-matched InAlN electron blocking layer in green light-emitting diodes. *Appl Phys Lett*, 2010, 96: 101102
- [30] Choi S, Kim H J, Kim S S, et al. Improvement of peak quantum efficiency and efficiency droop in III-nitride visible light-emitting diodes with an InAlN electron-blocking layer. *Appl Phys Lett*, 2010, 96: 221105
- [31] Wang C H, Ke C C, Lee C Y, et al. Hole injection and efficiency droop improvement in InGaN/GaN light-emitting diodes by band-engineered electron blocking layer. *Appl Phys Lett*, 2010, 97: 261103
- [32] Kuo Y K, Chang J Y, Tsai M C. Enhancement in hole-injection efficiency of blue InGaN light-emitting diodes from reduced polarization by some specific designs for the electron blocking layer. *Opt Lett*, 2010, 35: 3285
- [33] Zhang Y, Kao T T, Liu J, et al. Effects of a step-graded $\text{Al}_x\text{Ga}_{1-x}\text{N}$ electron blocking layer in InGaN-based laser diodes. *J Appl Phys*, 2011, 109: 083115
- [34] Guo Yao, Liang Meng, Fu Jiajia, et al. Enhancing the performance of blue GaN-based light emitting diodes with double electron blocking layers. *AIP Adv*, 2015, 5: 037131
- [35] Ren Peng, Zhang Ning, Liu Zhe, et al. Promotion of electron confinement and hole injection in GaN-based green light-emitting diodes with a hybrid electron blocking layer. *J Phys D*, 2015, 48: 045101
- [36] Liu Zhiqiang, Ma Jun, Yi Xiaoyan, et al. p-InGaN/AlGaN electron blocking layer for InGaN/GaN blue light-emitting diodes. *Appl Phys Lett*, 2012, 101: 261106
- [37] Zhang Ning, Liu Zhe, Wei Tongbo, et al. Effect of the graded electron blocking layer on the emission properties of GaN-based green light-emitting diodes. *Appl Phys Lett*, 2012, 100: 053504
- [38] Adivarahan V, Heidari A, Zhang B, et al. Vertical injection thin film deep ultraviolet light emitting diodes with AlGaN multiple-quantum wells active region. *Appl Phys Express*, 2009, 2: 092102
- [39] Huang H W, Lin C H, Yu C C, et al. Investigation of GaN-based vertical-injection light-emitting diodes with GaN nano-cone structure by ICP etching. *Mater Sci Eng B*, 2008, 151: 205
- [40] Wang L, Zhang Y, Li X, et al. Partially sandwiched graphene as transparent conductive layer for InGaN-based vertical light emitting diodes. *Appl Phys Lett*, 2012, 101: 061102
- [41] Rozhansky I V, Zakheim D A. Analysis of processes limiting quantum efficiency of AlGaN LEDs at high pumping. *Physica Status Solidi*, 2007, 204(1): 227
- [42] Xie Jinqiao, Ni Xianfeng, Fan Qian, et al. On the efficiency droop in InGaN multiple quantum well blue light emitting diodes and its reduction with p-doped quantum well barriers. *Appl Phys Lett*, 2008, 93(12): 121107
- [43] Kim J, Bayram C, Park H, et al. Principle of direct van der Waals epitaxy of single-crystalline films on epitaxial graphene. *Nat Commun*, 2014, 5: 4836
- [44] Kuo Y K, Chang J Y, Tsai M C. Enhancement in hole-injection efficiency of blue InGaN light-emitting diodes from reduced polarization by some specific designs for the electron blocking layer. *Opt Lett*, 2010, 35(19): 3285
- [45] Amano H, Kito M, Hiramatsu K, et al. P-type conduction in Mg-doped GaN treated with low-energy electron-beam irradiation (Leebi). *Jpn J Appl Phys*, 1989, 28(12): 2112
- [46] Nakamura S, Iwasa N, Senoh M, et al. Hole compensation mechanism of p-type GaN films. *Jpn J Appl Phys*, 1992, 31(5a): 1258
- [47] Wei Tongbo, Duan Ruifei, Wei Xuecheng, et al. Hydride vapor phase epitaxy growth of semipolar (1013) GaN on patterned m-plane sapphire. *J Electrochemical Soc*, 2010, 157(7): 721
- [48] Simon J, Protasenko V, Jena D, et al. Polarization-induced hole doping in wide-band-gap uniaxial semiconductor heterostructures. *Science*, 2010, 327(5961): 60
- [49] Zhang Lian, Wei Xuecheng, Lu Hongxi, et al. Improvement of efficiency of GaN-based polarization-doped light-emitting diodes grown by metal organic chemical vapor deposition. *Appl Phys Lett*, 2011, 98(24): 241111
- [50] Zhang Lian, Wei Tongbo, Ma Ping, et al. Theoretical study of polarization-doped GaN-based light-emitting diodes. *Appl Phys Lett*, 2011, 98(10): 101
- [51] Liu Zhiqiang, Yi Xiaoyan, Yu Zhiguo, et al. Impurity resonant states p-type doping in wide-band-gap nitrides. *Sci Rep*, 2016, 6: 19537
- [52] Liu Zhiqiang, Fu Binglei, Yi Xiaoyan, et al. Co-doping of magnesium with indium in nitrides: first principle calculation and experiment. *RSC Adv*, 2016, 6(6): 5111
- [53] Tchernycheva M, Lavenus P, Zhang H, et al. InGaN/GaN core-shell single nanowire light emitting diodes with graphene-based p-contact. *Nano Lett*, 2014, 14(5): 2456
- [54] Riley J R, Padalkar S, Li Q, et al. Three-dimensional mapping of quantum wells in a GaN/InGaN core-shell nanowire light-emitting diode array. *Nano Lett*, 2013, 13(9): 4317
- [55] Nguyen H P, Zhang S, Connie A T, et al. Breaking the carrier injection bottleneck of phosphor-free nanowire white light-emitting diodes. *Nano Lett*, 2013, 13(11): 5437
- [56] Koester R, Hwang J S, Salomon D, et al. *M*-plane core-shell InGaN/GaN multiple-quantum-wells on GaN wires for electroluminescent devices. *Nano Lett*, 2011, 11(11): 4839
- [57] Qian F, Gradecak S, Li Y, et al. Core/multishell nanowire heterostructures as multicolor, high-efficiency light-emitting diodes. *Nano Lett*, 2005, 5(11): 2287
- [58] Waltereit P, Brandt O, Trampert A, et al. Nitride semiconductors free of electrostatic fields for efficient white light-emitting diodes. *Nature*, 2000, 406(6798): 865
- [59] Chang S P, Chen Y C, Huang J K, et al. Electrically driven nanoparamid green light emitting diode. *Appl Phys Lett*, 2012, 100(6): 061106
- [60] Li S F, Waag A. GaN based nanorods for solid state lighting. *J Appl Phys*, 2012, 111(7): 071101
- [61] Hersee S D, Sun X Y, Wang X. The controlled growth of GaN nanowires. *Nano Lett*, 2006, 6(8): 1808
- [62] Jung B O, Bae S Y, Kato Y, et al. Morphology development of GaN nanowires using a pulsed-mode MOCVD growth technique. *Cryst Eng Comm*, 2014, 16(11): 2273
- [63] Ma Jun, Wang Liancheng, Liu Zhiqiang, et al. Nitride-based micron-scale hexagonal pyramids array vertical light emitting diodes by N-polar wet etching. *Opt Express*, 2013, 21(3): 3547

- [64] Wang Liancheng, Ma Jun, Liu Zhiqiang, et al. N-polar GaN etching and approaches to quasi-perfect micro-scale pyramid vertical light-emitting diodes array. *J Appl Phys*, 2013, 114(13): 133101
- [65] Kang Junjie, Li Zhi, Liu Zhiqiang, et al. Investigation of the wet-etching mechanism of Ga-polar AlGaN/GaN micro-pillars. *J Cryst Growth*, 2014, 386: 175
- [66] Ren Peng, Han Gang, Fu Binglei, et al. Selective area growth and characterization of GaN nanorods fabricated by adjusting the hydrogen flow rate and growth temperature with metal organic chemical vapor deposition. *Chin Phys Lett*, 2016, 33(6): 068101
- [67] Wu Kui, Wei Tongbo, Lan Ding, et al. Phosphor-free nanoparamid white light-emitting diodes grown on {1011} planes using nanospherical-lens photolithography. *Appl Phys Lett*, 2013, 103(24): 241107
- [68] Kang Junjie, Li Zhi, Li Hongjian, et al. Pyramid array InGaN/GaN core-shell light emitting diodes with homogeneous multilayer graphene electrodes. *Appl Phys Express*, 2013, 6(7): 072102
- [69] Wang Liancheng, Zhang Yiyun, Li Xiao, et al. Partially sandwiched graphene as transparent conductive layer for InGaN-based vertical light emitting diodes. *Appl Phys Lett*, 2012, 101(6): 061102
- [70] Wang Liancheng, Liu Wei, Zhang Yiyun, et al. Graphene-based transparent conductive electrodes for GaN-based light emitting diodes: challenges and countermeasures. *Nano Energy*, 2015, 12: 419
- [71] Park T Y, Choi Y S, Kang J W, et al. Enhanced optical power and low forward voltage of GaN-based light-emitting diodes with Ga-doped ZnO transparent conducting layer. *Appl Phys Lett*, 2010, 96(5): 051124
- [72] Kuang P, Park J M, Leung W, et al. A new architecture for transparent electrodes: relieving the trade-off between electrical conductivity and optical transmittance. *Adv Mater*, 2011, 23(21): 2469
- [73] Rowell M W, Topinka M A, McGehee M D, et al. Organic solar cells with carbon nanotube network electrodes. *Appl Phys Lett*, 2006, 88(23): 233506
- [74] Wu Junbo, Becerril H A, Bao Zhenan, et al. Organic solar cells with solution-processed graphene transparent electrodes. *Appl Phys Lett*, 2008, 92(26): 263302
- [75] Zhang Yiyun, Wang Liancheng, Li Xiao, et al. Annealed InGaN green light-emitting diodes with graphene transparent conductive electrodes. *J Appl Phys*, 2012, 111(11): 114501
- [76] Wang Liancheng, Zhang Yiyun, Li Xiao, et al. Interface and transport properties of GaN/graphene junction in GaN-based LEDs. *J Phys D*, 2012, 45(50): 505102
- [77] Wang Liancheng, Zhang Yiyun, Li Xiao, et al. Improved transport properties of graphene/GaN junctions in GaN-based vertical light emitting diodes by acid doping. *RSC Adv*, 2013, 3(10): 3359
- [78] Li Zhi, Kang Junjie, Liu Zhiqiang, et al. Enhanced performance of GaN-based light-emitting diodes with graphene/Ag nanowires hybrid films. *AIP Ad*, 2013, 3(4): 042134
- [79] Zhang Yiyun, Li Xiao, Wang Liancheng, et al. Enhanced light emission of GaN-based diodes with a NiO_x/graphene hybrid electrode. *Nanoscale*, 2012, 4(19): 5852
- [80] Li Zhi, Kang Junjie, Zhang Yiyun, et al. The fabrication of GaN-based nanorod light-emitting diodes with multilayer graphene transparent electrodes. *J Appl Phys*, 2013, 113(23): 234302
- [81] Fu Binglei, Cheng Yan, Si Zhao, et al. Phosphor-free InGaN micro-pyramid white light emitting diodes with multilayer graphene electrode. *RSC Adv*, 2015, 5(122): 100646
- [82] Tian Ting, Zhan Teng, Guo Jinxia, et al. Transparent graphene interconnects for monolithic integration of GaN-based LEDs. *Appl Phys Express*, 2015, 8(4): 042102
- [83] Utama M I, Zhang Q, Zhang J, et al. Recent developments and future directions in the growth of nanostructures by van der Waals epitaxy. *Nanoscale*, 2013, 5(9): 3570
- [84] Chung K, Park S I, Baek H, et al. High-quality GaN films grown on chemical vapor-deposited graphene films. *NPG Asia Materials*, 2012, 4(9): e24
- [85] Gupta P, Rahman A A, Hatui N, et al. MOVPE growth of semipolar III-nitride semiconductors on CVD graphene. *J Cryst Growth*, 2013, 372: 105
- [86] Kim J, Bayram C, Park H, et al. Principle of direct van der Waals epitaxy of single-crystalline films on epitaxial graphene. *Nat Commun*, 2014, 5: 4836
- [87] Al Balushi Z Y, Miyagi T, Lin Y C, et al. The impact of graphene properties on GaN and AlN nucleation. *Surface Science*, 2015, 634: 81
- [88] Chae S J, Kim Y H, Seo T H, et al. Direct growth of etch pit-free GaN crystals on few-layer graphene. *RSC Adv*, 2015, 5(2): 1343